## Appendix B: Non detection spectras

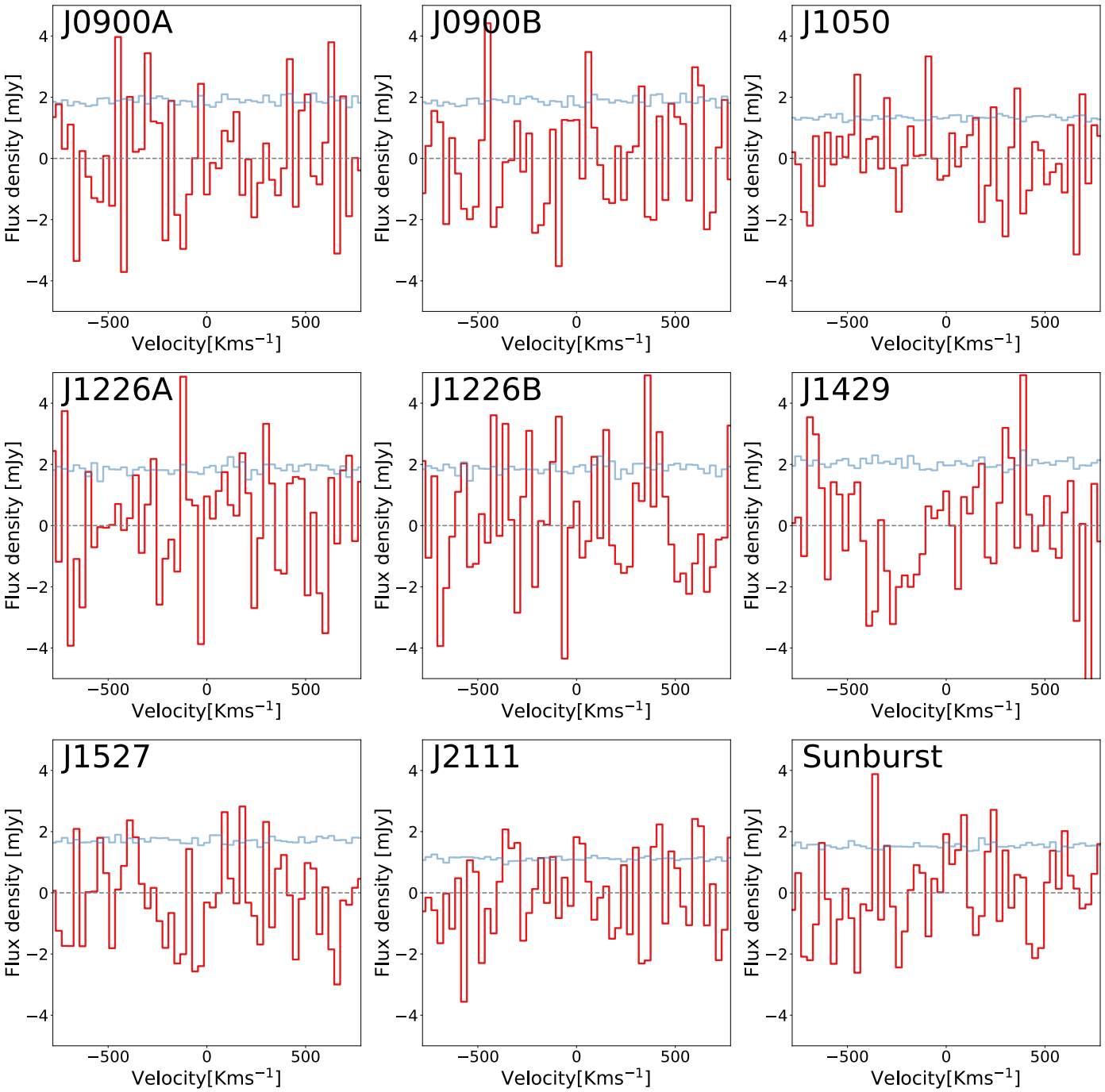


Fig. B.1: Spectrum of arcs, where the red line indicates the spectrum and the blue line a $1\sigma$ error

## Appendix C: SED fits

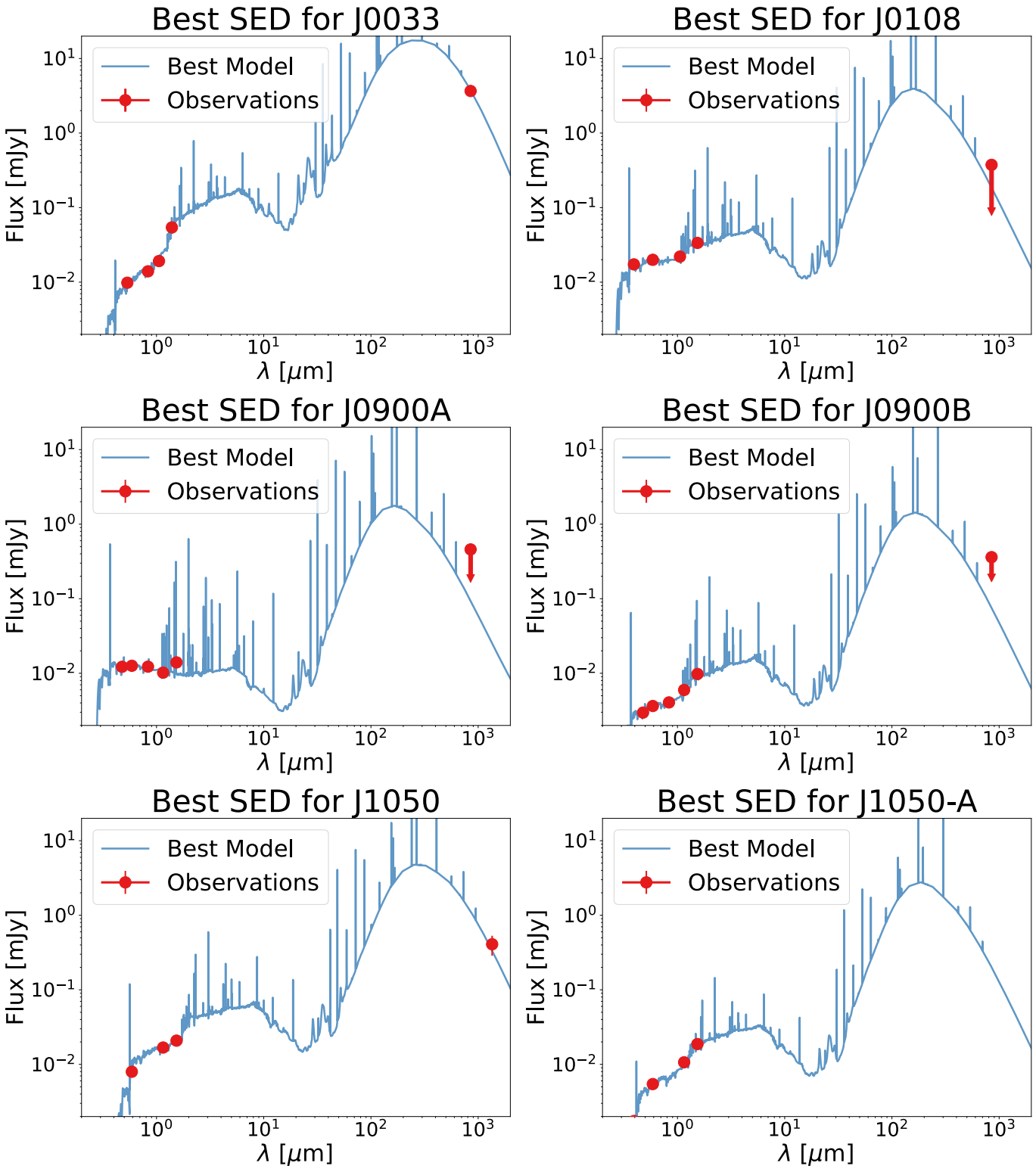


Fig. C.1: SED fit for the gravitational arcs using HST and ALMA photometry, modeled with CIGALE to derive the physical properties.

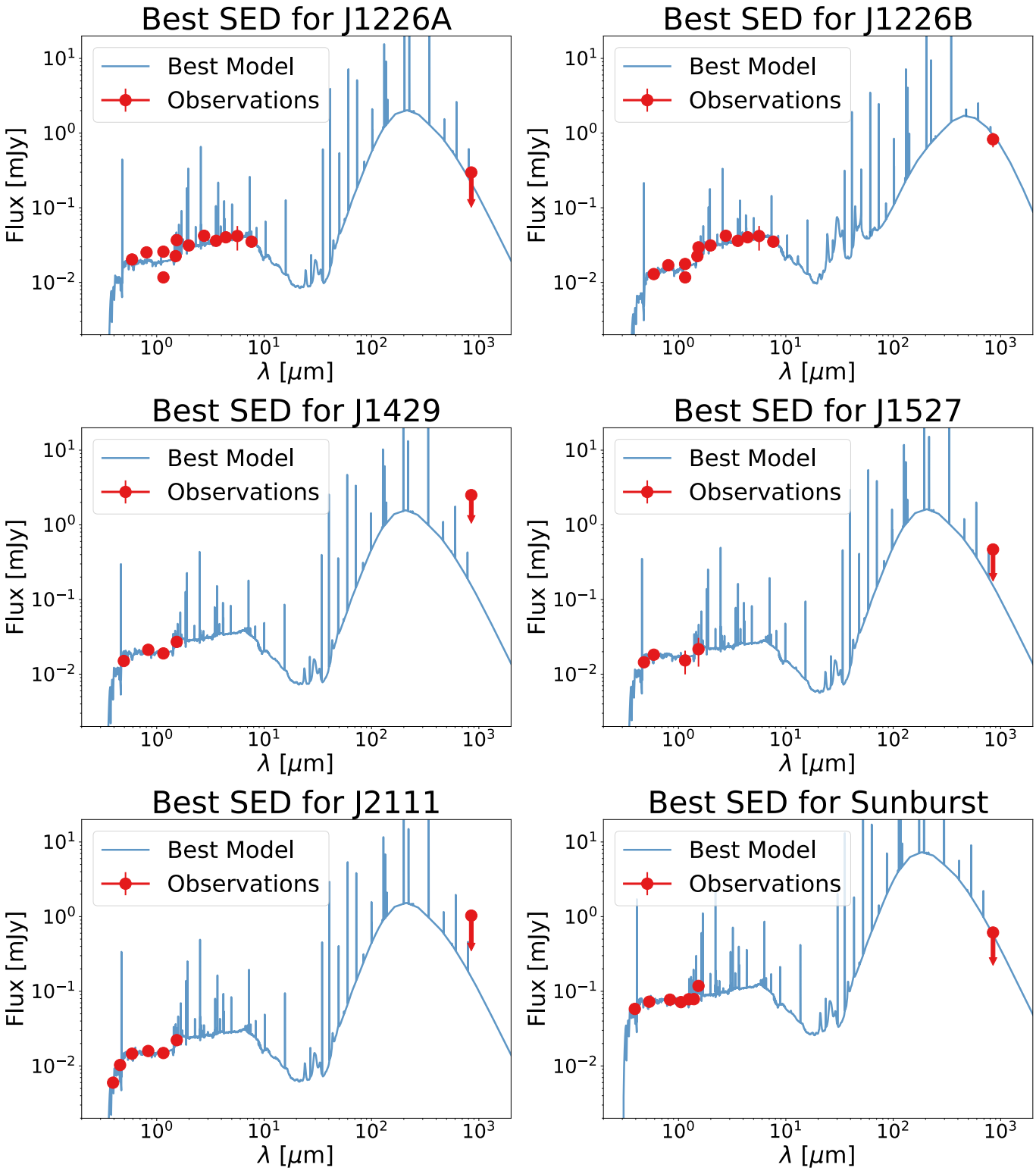


Fig. C.2: Continuation of Fig. C.1

## Appendix D: Data for $r_{J1}$

Table D.1: The dataset utilized for developing models linking ΣSFR and $r_{J1}$

| Galaxy | $z$ | $\Sigma_{SFR}$ [$M_\odot yr^{-1} kpc^{-2}$] | $r_{31}$ | $r_{41}$ | $r_{51}$ | Reference |
|---|---|---|---|---|---|---|
| D13-5 | 0.075 | 0.066 | 0.55±0.02 | 0.32±0.01 | - | 1 |
| D15-3 | 0.067 | 0.024 | - | 0.16±0.01 | - | 1 |
| G04-1 | 0.130 | 0.02 | 0.54±0.04 | 0.28±0.02 | - | 1 |
| G08-5 | 0.140 | 0.02 | 0.8 ±0.1 | - | - | 1 |
| G14-1 | 0.132 | 0.02 | 0.48±0.08 | 0.27±0.03 | - | 1 |
| G20-2 | 0.141 | 0.04 | 0.58±0.07 | 0.33±0.04 | - | 1 |
| AS2COS0023.1 | 4.341 | 161.96±28.00 | - | 1.26±0.56 | - | 2 |
| AS2UDS011.0* | 4.073 | 587.80±251.10 | - | 1.46±0.93 | - | 2 |
| AS2UDS026.0 | 3.296 | 73.71±31.50 | - | 1.22±0.51 | - | 2 |
| CDFN8 | 4.144 | 117.10±41.00 | - | 1.07±0.38 | - | 2 |
| AS2COS0031.1 | 3.643 | 27.28±9.30 | - | 0.51±0.15 | - | 2 |
| AS2COS0054.1 | 3.174 | 130.00±32.80 | - | 0.42±0.18 | - | 2 |
| AS2COS0008.1 | 3.581 | 161.00±28.90 | - | 0.63±0.22 | - | 2 |
| CDFN2 | 4.422 | 252.20±67.50 | - | 0.59±0.18 | - | 2 |
| AS2UDS012.0 | 2.520 | 46.70±8.30 | 0.37±0.11 | - | - | 2 |
| AS2UDS010.0 | 3.169 | 99.10±30.90 | 0.6±0.18 | - | - | 2 |
| AS2COS0013.1 | 2.608 | 95.40±21.60 | 1.16±0.24 | - | - | 2 |
| CDFN1 | 3.159 | 168.80±46.20 | 0.31±0.09 | - | - | 2 |
| AS2UDS126.0 | 2.436 | 467.10±382.90 | 0.9±0.56 | - | - | 2 |
| HOSTGALAXY GRB080207 | 2.086 | 3.40 | 1.098±1.09 | 0.988±1.02 | - | 3 |
| arp 220 | 0.018 | 411.10 | 0.97±0.14 | - | - | 4,5 |
| NGC 6240 | 0.024 | 4.94 | 1.1±0.24 | - | - | 4,5 |
| NGC 7469 | 0.016 | 11.32 | 0.6±0.1 | 0.83±0.19 | - | 4,5 |
| Zw 049.057 | 0.013 | 22.59 | 0.66±0.11 | 0.58±0.15 | - | 4,5 |
| arp 193 | 0.023 | 149.26 | 0.74±0.12 | - | - | 4,5 |
| NGC 1068 | 0.004 | 210.84 | 0.67±0.16 | - | - | 4,5 |
| B1228-113 | 2.193 | 1.79 | 0.86±0.21 | - | - | 6 |
| j0918+1636 | 2.585 | 6.21 | 1.0±0.2 | 1.03±0.23 | 0.39 | 6 |
| BzK-4171 | 1.465 | 0.80 | 0.47±0.15 | - | 0.37 | 7 |
| BzK-16000 | 1.525 | 0.82 | 0.27±0.07 | - | 0.12 | 7 |
| BzK-21000 | 1.521 | 1.68 | 0.57±0.14 | - | 0.36 | 7 |
| HFLS3 | 6.340 | 600.00 | 1.08±0.17 | - | - | 8 |
| BX610 | 2.200 | 1.61 | 0.92±0.17 | 1.08±0.22 | - | 9 |
| MD94 | 2.000 | 1.89 | 1.21±0.13 | - | - | 10 |

**References.** (1) Lenkić et al. (2023),(2) Castillo et al. (2023),(3) Hatsukade et al. (2019),(4) Taniguchi & Ohyama (1998),(5) Papadopoulos et al. (2012),(6) Kaur et al. (2022),(7) Daddi et al. (2015),(8) Riechers et al. (2013),(9) Brisbin et al. (2019) ,(10) Henríquez-Brocal et al. (2022)

## Appendix E: Cigale Parameters

This section outlines the parameters employed in running CIGALE. Constant parameters are detailed in Table E.1, while variable parameters are listed in Table E.2.

Table E.1: CIGALE parameters that remained constant across all arcs.

| Module | Parameter | Values |
|---|---|---|
| bc03 | | |
| | imf | 0 |
| | metallicity | 0.02 |
| | separation_age | 10 |
| dustatt_modified_CF00 | | |
| | Av_ISM | "eval np.arange(0,2,0.05)" |
| | mu | 0.44 |
| | slope_ISM | -0.7 |
| | slope_BC | -1.3 |
| | filters | V_B90,FUV |
| nebular | | |
| | logU | -2.0 |
| | zgas | 0.02 |
| | ne | 100 |
| | f_esc | 0.0 |
| | lines_width | 300 |
| | emission | True |
| dale2014 | | |
| | fracAGN | 0 |
| | alpha | 0.0625,0.5000,1.0000, 1.5000, 2.0000<br>2.5000, 3.0000, 3.5000, 4.0000 |
| sfhdelayed | | |
| | sfr_A | 1.0 |
| | normalize | True |
| | tau_main | 2000 |
| | f_burst | 0, 0.01, 0.05, 0.1,0.25 |
| restframe_parameters | | |
| | beta_calz94 | True |
| | D4000 | False |
| | IRX | False |
| | luminosity_filters | FUV, V_B90 |
| | colours_filters | FUV-NUV, NUV-r_prime |

Table E.2: Variations in CIGALE parameters utilized for each arc.

| Arc | Module | Parameter | Values |
|---|---|---|---|
| 0033 | sfhdelayed | | |
| | | age_main | 1000,1500,2000,2500 |
| | | tau_burst | 10, 25, 50, 100, 250, 500 |
| | | age_burst | 25, 50, 100, 250,500,1000 |
| 0108 | sfhdelayed | | |
| | | age_main | 500,1000,2000,2200 |
| | | tau_burst | 10, 25, 50, 100, 250, 500 |
| | | age_burst | 25, 50, 100, 250,500 |
| 0900 | sfhdelayed | | |
| | | age_main | 500, 1000, 1500, 2000, 2500,3000 |
| | | tau_burst | 10, 25, 50, 100, 250, 500 |
| | | age_burst | 25, 50, 100, 250,500 |
| 1050 | sfhdelayed | | |
| | | age_main | 500,1000,1500 |
| | | tau_burst | 10, 25, 50, 100, 250 |
| | | age_burst | 25, 50, 100, 250,500 |
| 1050A | sfhdelayed | | |
| | | age_main | 500,1000,1500,2000,2500 |
| | | tau_burst | 10, 25, 50, 100, 250, 500 |
| | | age_burst | 25, 50, 100, 250,500 |
| 1226 | sfhdelayed | | |
| | | age_main | 200,500,1000,1200, 1800 |
| | | tau_burst | 10, 25, 50, 100, 250, 500, 1000 |
| | | age_burst | 25, 50, 100 |
| 1429 | sfhdelayed | | |
| | | age_main | 100,500,1000,1750,2080 |
| | | tau_burst | 10, 25, 50, 100, 250, 500 |
| | | age_burst | 25, 50, 100 |
| 1527 | sfhdelayed | | |
| | | age_main | 100,500,1000,1750,2000, 2300 |
| | | tau_burst | 10, 25, 50, 100, 250, 500 |
| | | age_burst | 25, 50, 100 |
| 2111 | sfhdelayed | | |
| | | age_main | 100,500,1000,1750,2050 |
| | | tau_burst | 10, 25, 50, 100, 250, 500 |
| | | age_burst | 25, 50, 100 |
| Sunburst | sfhdelayed | | |
| | | age_main | 1000,1500,2000,2500 |
| | | tau_burst | 10, 25, 50, 100, 250, 500 |
| | | age_burst | 25, 50, 100, 250,500,1000 |

## Appendix F: Flux percentages

Table F.1: Percentage of total flux covered in HST apertures

| Arc | Percentage |
|---|---|
| J0033 | 97% |
| J0108 | 99% |
| J0900A | 95% |
| J0900B | 94% |
| J1050 | 91% |
| J1050-A | 91% |
| J1226A | 90% |
| J1226B | 90% |
| J1429 | 93% |
| J1527 | 93% |
| J2111 | 96% |
| Sunburst | 92% |